Biochimica et Biophysica Acta 1843 (2014) 1899–1908

Contents lists available at ScienceDirect

Biochimica et Biophysica Acta

journal homepage: www.elsevier.com/locate/bbamcr

Functional expression of adrenoreceptors in mesenchymal stromal cells derived from the human adipose tissue

Polina D. Kotova [a], Veronika Yu. Sysoeva [b], Olga A. Rogachevskaja [a], Marina F. Bystrova [a], Alisa S. Kolesnikova [a], Pyotr A. Tyurin-Kuzmin [b], Julia I. Fadeeva [b], Vsevolod A. Tkachuk [b], Stanislav S. Kolesnikov [a,*]

[a] Institute of Cell Biophysics, Russian Academy of Sciences, Pushchino, Moscow Region 142290, Russia
[b] Department of Biochemistry and Molecular Medicine, Faculty of Basic Medicine, Lomonosov Moscow State University, Russia

ARTICLE INFO

Article history:
Received 1 March 2014
Received in revised form 1 May 2014
Accepted 9 May 2014
Available online 16 May 2014

Keywords:
Mesenchymal stromal cell
Adrenergic receptor
Calcium-induced calcium release
Ca^{2+} uncaging
IP_3 receptor

ABSTRACT

Cultured mesenchymal stromal cells (MSCs) from different sources represent a heterogeneous population of proliferating non-differentiated cells that contains multipotent stem cells capable of originating a variety of mesenchymal cell lineages. Despite tremendous progress in MSC biology spurred by their therapeutic potential, current knowledge on receptor and signaling systems of MSCs is mediocre. Here we isolated MSCs from the human adipose tissue and assayed their responsivity to GPCR agonists with Ca^{2+} imaging. As a whole, a MSC population exhibited functional heterogeneity. Although a variety of first messengers was capable of stimulating Ca^{2+} signaling in MSCs, only a relatively small group of cells was specifically responsive to the particular GPCR agonist, including noradrenaline. RT-PCR and immunocytochemistry revealed expression of α1B-, α2A-, and β2-adrenoreceptors in MSCs. Their sensitivity to subtype-specific adrenergic agonists/antagonists and certain inhibitors of Ca^{2+} signaling indicated that largely the α2A-isoform coupled to PLC endowed MSCs with sensitivity to noradrenaline. The all-or-nothing dose-dependence was characteristic of responsivity of robust adrenergic MSCs. Noradrenaline never elicited small or intermediate responses but initiated large and quite similar Ca^{2+} transients at all concentrations above the threshold. The inhibitory analysis and Ca^{2+} uncaging implicated Ca^{2+}-induced Ca^{2+} release (CICR) in shaping Ca^{2+} signals elicited by noradrenaline. Evidence favored IP_3 receptors as predominantly responsible for CICR. Based on the overall findings, we inferred that adrenergic transduction in MSCs includes two fundamentally different stages: noradrenaline initially triggers a local and relatively small Ca^{2+} signal, which next stimulates CICR, thereby being converted into a global Ca^{2+} signal.

1. Introduction

Apart from fully differentiated cells, apparently all postnatal mammalian tissues contain rare and quiescent stem cells that have the capacity for self-renewal and initiating differentiated descendants [1,2]. Mesenchymal stem cells are an uncommon population present in the bone marrow and tissues, such as the adipose tissue, synovium, dermis, periosteum, and deciduous teeth. During isolation and expansion in vitro mesenchymal stem cells constitute a minor fraction (<1%) of the total mesenchymal stromal cell (MSC) population. The increasing body of evidence points to the intrinsic, and donor-to-donor heterogeneity of MSC populations [3–5]. One of the pioneering demonstrations of populational diversity was provided by the microSAGE assay of MSC colonies derived from a single human bone marrow cell. The expression analysis revealed transcripts for more than 2000 genes encoding proteins known to regulate angiogenesis, cell motility, hematopoiesis, immunity, and neural activities [6,7]. It seems to be highly unlikely if an individual cell would be capable of fulfilling all these autonomous physiological functions. Consistently, immunostaining data suggested a non-uniform pattern of protein expression [7]. It was therefore postulated that a variety of functional attributes characteristic of the entire MSC population was determined by separate subpopulations. The concept of intrinsic heterogeneity of a MSC population is well consistent with the finding that a MSC colony can release a broad array of signaling molecules, including FGF-2, BDNF, IGF1, ANG1 and certain cytokines and chemokines [8]. Although mammalian MSCs are poorly characterized in terms of intracellular signaling and ionic mechanisms of electrogenesis, available reports also evidence for molecular and functional heterogeneity of MSC populations [9,10].

Several key factors determine cell proliferation and differentiation, including intrinsic genetic programs, intracellular signaling, and local environmental cues. Reportedly, spontaneous Ca^{2+} oscillations and induced Ca^{2+} transients can mediate development, from fertilization through proliferation and differentiation to organogenesis, and expansion of progenitor pools [11–13]. Thus, membrane receptors and regulatory

* Corresponding author at: Institute of Cell Biophysics, Russian Academy of Sciences, Institutional Street 3, Pushchino, Moscow Region 142290, Russia. Tel.: +7 96 773 9121; fax: +7 96 733 0509.
E-mail address: staskolesnikov@yahoo.com (S.S. Kolesnikov).

http://dx.doi.org/10.1016/j.bbamcr.2014.05.002
0167-4889/

pathways associated with intracellular Ca^{2+} signaling can be critically important for tissue development and regeneration. Although a role of ion channels is much less obvious, they may also be involved in coordinating extracellular and intracellular signals associated with cell proliferation and differentiation [10,14–16]. Specifically, ion channels can regulate exocytosis of autocrine and paracrine factors by determining membrane potential and Ca^{2+} influx [16]. Transmembrane ion fluxes drive cell volume oscillations in cycling and migrating cells [17,18]. Yet, ion channels are capable of modulating cell proliferation and differentiation via flux-independent mechanisms, including association of channel proteins with membrane receptors and related proteins [19–22].

In light of molecular and functional heterogeneity of a MSC population posed by the abovementioned facts, the important possibility is that molecular and functional phenotypes of these cells may be in strong correlation. If so, an individual MSC subpopulation with a specific molecular profile could be revealed physiologically and described in terms of responsivity to agonists, Ca^{2+} signaling pathways, and/or activity of ion channels. We therefore attempted to characterize responsiveness of adipose-derived human MSCs to a variety of agonists, such as ACh, ATP, noradrenaline, serotonin, and some others, which are known to mobilize cytosolic Ca^{2+} in cells of diverse types. All first messengers probed by us were found to stimulate Ca^{2+} signaling in MSCs. Since apart from ATP, a given cell usually responded to one of them, it appears that different MSC subpopulations can indeed be classified based on functional criteria. Here we focused largely on the analysis of MSCs responsive to noradrenaline, given some interesting aspects of Ca^{2+} signaling in adrenergic cells.

2. Materials and methods

2.1. Cell isolation and culturing

Human MSCs were isolated from abdominal subcutaneous adipose tissue harvested during surgical operations from patients at age within 32–60 years. All donors gave informed consent for harvesting their adipose tissue. Donors with infectious or systemic diseases and malignancies were not included in the study. Adipose tissue was extensively washed with 2 volumes of Hank's Balanced Salt Solution (HBSS) containing 1% antibiotic/antimycotic solution (HyClone) and then digested at 37 °C for 1 h in the presence of collagenase (66.7 U/ml, Sigma-Aldrich) and dispase (10 U/ml, BD Biosciences). Enzymatic activity was neutralized by adding an equal volume of culture medium (AdvanceStem basal medium for human undifferentiated mesenchymal stem cells (HyClone) containing 10% of Advance stem cell growth supplement (CGS) (HyClone), 1% antibiotic/antimycotic solution) and centrifuged at 200 *g* for 10 min. This led to sedimentation of diverse cells, including MSCs, macrophages, lymphocytes, and erythrocytes, while mature adipocytes remained floating. After removal of supernatant, a lysis solution (154 mM NH_4Cl, 10 mM $KHCO_3$, and 0.1 mM EDTA) was added to a cell pellet to lyse erythrocytes, and cell suspension was centrifuged at 200 *g* for 10 min. Sedimented cells were resuspended in the MSC culture medium and filtered through a 100 μm nylon cell strainer (BD Biosciences). As indicated by flow cytometry data (Supplementary Materials, Fig. 1S), after isolation and overnight pre-plating, the obtained cell population contained largely not only MSC cells but also macrophages and lymphocytes. The two last cell groups were dramatically depleted by culturing during 1 week in the MSC culture medium and humidified atmosphere (5% CO_2) at 37 °C. The obtained MSC population was maintained at a sub-confluent level (<80% confluency) and passaged using HyQTase (HyClone). For experiments, cells of the second to fourth passages were used.

2.2. Preparation of cells for Ca^{2+} imaging

Before assaying with Ca^{2+} imaging, cells were maintained in a 12-socket plate for 12 h in the medium described above but without antibiotics. For isolation, cells cultured in a 1 ml socket were rinsed twice with the Versen solution (Sigma-Aldrich) that was then substituted for 0.2 ml HyQTase solution (HyClone) for 3–5 min. The enzymatic treatment was terminated by the addition of a 0.8 ml culture medium to a socket. Next, cells were resuspended, put into a tube, and centrifuged at 0.8 *g* for 45 s for sedimentation. Isolated cells were collected by a plastic pipette and plated onto a recording chamber of nearly 150 μl volume. The last was a coverslip (Menzel-Glaser) with attached ellipsoidal resin wall. The chamber bottom was coated with Cell-Tak (BD Biosciences) allowing for strong cell adhesion. Attached cells were then loaded with dyes at room temperature (23–25 °C) by adding Fluo-4AM (4 μM) or Fluo-4AM (4 μM) + NP-EGTA-AM (4 μM) and Pluronic (0.02%) (all from Molecular Probes) to the bath solution (mM): NaCl — 110, KCl — 5.5, $CaCl_2$ — 2, $MgSO_4$ — 0.8, HEPES — 10, and glucose — 10, pH 7.4. After 20-min incubation cells were rinsed several times with the bath solution and stored at 4 °C for 40 min. When necessary, 2 mM $CaCl_2$ in the bath solution was replaced with 0.5 mM EGTA + 0.4 mM $CaCl_2$, thus reducing free Ca^{2+} to nearly 260 nM.

2.3. Ca^{2+} imaging and uncaging

Most of experiments were carried out using an inverted fluorescent microscope Axiovert 135 equipped with an objective Plan NeoFluar 20x/0.75 (Zeiss) and a digital ECCD camera LucaR (Andor Technology). Apart from a transparent light illuminator, the microscope was equipped with a hand-made system for epi-illumination via an objective. The epi-illumination was performed using a bifurcational glass fiber. One channel, which was used for Fluo-4 excitation, transmitted 480 ± 5 nm irradiation emitted by LED controlled by a computer. Fluo-4 emission was collected at 535 ± 20 nm. Serial fluorescent images were captured every second and analyzed using Imaging Workbench 6 software (INDEC). Deviations of cytosolic Ca^{2+} from the resting level were quantified by a relative change in the intensity of Fluo-4 fluorescence ($\Delta F/F_0$) recorded from an individual cell. Another channel was connected to a pulsed solid laser DTL-374QT (30 mW) (Laser-Export, Moscow). This unit operated in a two-harmonic mode and generated not only 355 nM UV light used for Ca^{2+} uncaging but also visible light at 532 nm. The last could penetrate into an emission channel through non-ideal optical filters and elicited optical artifacts during uncaging. For Ca^{2+} uncaging, cells were loaded with both 4 μM Fluo-4 and NP-EGTA (both from Invitrogen). Other compounds were from Sigma-Aldrich or Tocris.

2.4. Immunofluorescent analysis

For immunofluorescence analysis cultured cells were washed with PBS and fixed in 4% formaldehyde for 4 min at room temperature. Cells were then washed with PBS. Nonspecific binding was blocked by incubation in 1% BSA with 10% serum of secondary antibody donor for 30 min. Immunostaining was performed using mouse antibody against human α1-adrenoreceptor (Abbiotec) and rabbit polyclonal antibody against the human α2-adrenoreceptor (Thermo Sci). Cells stained with primary antibodies were then incubated in the presence of secondary antibodies, Alexa goat anti-rabbit 488 (Molecular Probes, Carlsbad, CA) or Alexa goat anti-mouse 488 (Molecular Probes). Cells were counterstained with nuclear 4,6-diamidino-2-phenylindole (Molecular Probes). As a negative control, cells were treated with mouse or rabbit nonspecific IgGs at relevant concentrations. Immunofluorescence was captured using a Leica DM6000 microscope equipped with a Leica DFC360 FX camera and Las AF software (Leica).

2.5. RT-PCR

Total RNA was extracted from a sample containing 10^5–10^6 MSCs by using the RNeasy mini kit (Qiagen). Isolated RNA was treated with

DNase I (Ambion) and reverse-transcribed with Superscript III reverse transcriptase (Invitrogen), following the manufacturer's instruction. Obtained cDNA served as a template for PCR with gene-specific primers that were designed for all human adrenoreceptor genes and for some marker genes, including CD73, CD90, and CD105 (Supplementary Materials, Table 1S). The expected sizes of PCR products were as follows: 259 bp for ADRA1A (α1A), 379 bp for ADRA1B (α1B), 285 bp for ADRA1D (α1D), 347 bp for ADRA2A (α2A), 353 bp for ADRA2B (α2B), 291 bp for ADRA2C (α2C), 397 bp for ADRB1 (β1), 218 bp for ADRB2 (β2), 361 bp for ADRB3 (β3), 266 bp for CD73, 344 bp for CD90, and 300 bp for CD105.

3. Results

We loaded human MSCs with Fluo-4 and assayed their responsivity to different messengers using Ca^{2+} imaging. Functional heterogeneity was characteristic of MSCs. Although a variety of GPCR agonists was found to stimulate Ca^{2+} signaling in MSCs, in a whole MSC population, only a relatively small group of cells was specifically responsive to the particular agonist, including ATP, noradrenaline or adrenaline, serotonin, GABA, acetylcholine or its analog carbachol (Fig. 1), and glutamate (not shown). Basically, a given cell was either irresponsive to all stimuli or responded to one, rarely two, particular compound (Fig. 1A–E). When applied shortly, a given neurotransmitter typically triggered a Ca^{2+} transient in a responsive cell (Fig. 1A–E). Overall, 958 MSCs were sequentially stimulated by multiple agonists, and 302 cells (31%) responded to some of them. In a subpopulation of irresponsive MSCs, certain cells (2–5% depending on a sample) generated spontaneous Ca^{2+} oscillations under our recording conditions (Fig. 1F). ATP-sensitive cells (n = 112) composed the most abundant subgroup (37%), while adenosine and glutamate were the least effective agonists, being capable of mobilizing intracellular Ca^{2+} solely in 8 (2.6%) and 11 (3.6%) cells, respectively (Fig. 1G).

Here we focused on adrenergic signaling in MSCs. Because the effects of adrenaline and noradrenaline were identical, solely experiments with more frequently used noradrenaline are described below. Overall, more than 500 MSCs were distinguished by their ability to generate robust and reproducible Ca^{2+} transients on noradrenaline and its analogs. We first attempted to evaluate a part of Ca^{2+} release and Ca^{2+} entry, the primary contributors to intracellular Ca^{2+} signaling, in noradrenaline responses. It was particularly found that the inhibitor of phospholipase C (PLC) U73122 (1–5 μM) rendered MSCs insensitive to noradrenaline, while the much less effective analog U73343 never exerted such effects at concentrations of up to 10 μM (Fig. 2A) (n = 17). Besides, 2-APB known to inhibit IP_3 receptors damped noradrenaline responses as well (Fig. 2B) (n = 11). Note that 2-APB might also inhibit Ca^{2+} entry by exerting blockage of certain Ca^{2+}-permeable channels [23–25]. However, the reduction of bath Ca^{2+} from 2 mM to 260 nM influenced the sensitivity of adrenergic MSCs rather than the magnitude of noradrenaline responses (Fig. 2B, C). It thus appeared that in MSCs, the IP_3 receptor was a principal target for 2-APB. Indeed, overall 317 noradrenaline-sensitive MSCs were examined with normal (2 mM) and low (260 nM) Ca^{2+} in the bath. In all cases, MSC responses to saturating noradrenaline depended weakly or negligibly on the extracellular Ca^{2+}, while with 260 nM Ca^{2+} in the bath, cells became irresponsive at intermediate agonist concentrations (Fig. 2C). Thus, adrenergic transduction relies largely on Ca^{2+} release mediated by PLC and IP_3 receptors. Although bath Ca^{2+} somehow affected MSC sensitivity, to all appearance, Ca^{2+} entry determined the magnitude of noradrenaline responses to a little extent.

3.1. Dose–response curve

The interesting feature of adrenergic MSCs was that Ca^{2+} responses varied with noradrenaline concentration in a surprising "all-or-nothing" fashion (Fig. 3). In other words, noradrenaline never caused detectable

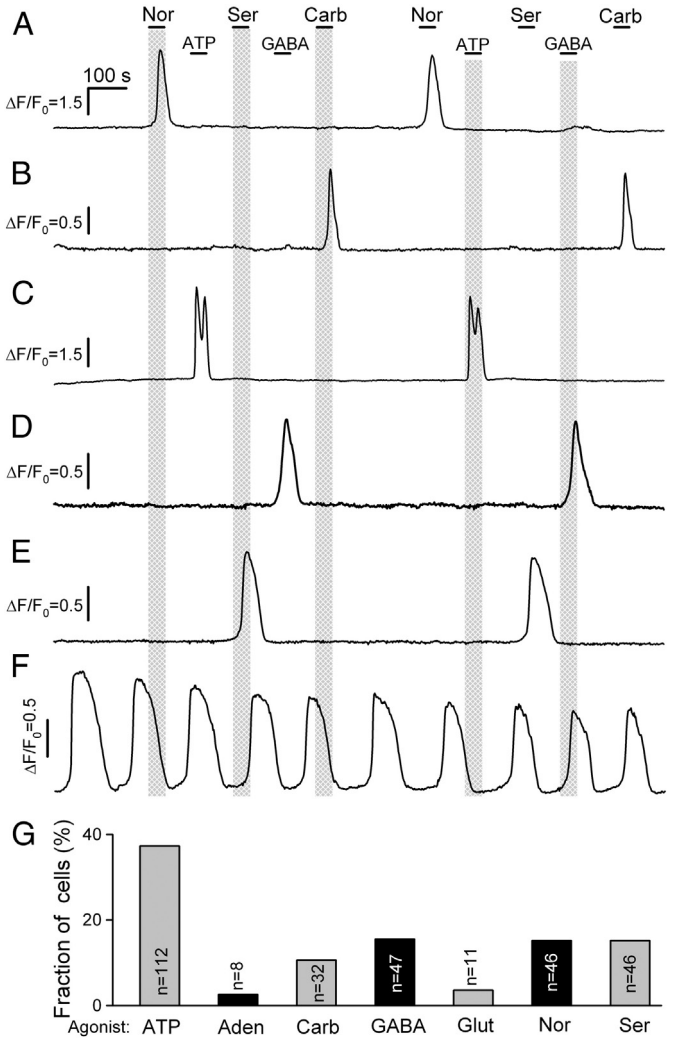

Fig. 1. Functional heterogeneity of mesenchymal stromal cells (MSCs) derived from the human adipose tissue. (A–E) Representative recordings of intracellular Ca^{2+} in Fluo-4 loaded cells and their responses to the particular agonist applied as indicated by the horizontal lines. (F) Representative recording from a cell generating spontaneous Ca^{2+} oscillations. In A–F, 6 different cells were assayed simultaneously; the shown traces are similarly scaled in time. (G) Fractional distribution of 302 MSCs, each being responsive to the particular agonist. Here, ATP — 10 μM adenosine triphosphate, Aden — 10 μM adenosine, Carb — 20 μM carbachol, GABA — 20 μM gamma-aminobutyric acid, Glut — 10 μM glutamic acid, Nor — 0.5 μM noradrenaline, Ser — 10 μM serotonin. Here and below, the data are presented as $\Delta F/F_0$, where $\Delta F = F - F_0$, F is the instant intensity of cell fluorescence, and F_0 is the intensity of cell fluorescence obtained in the very beginning of a recording and averaged over a 20-s interval.

effects, when applied below 100 nM, while at exceeding concentrations, it elicited marked Ca^{2+} transients of maximal or close magnitude in most cases (Fig. 3A, B). In designated experiments, we evaluated the dose–response curves of individual cells by stimulating them with noradrenaline at gradually varied concentrations. Among the 37 cells examined, 29 cells exhibited robust responses in the whole range of agonist concentrations (30 nM–10 μM) (e.g. Fig. 3B) with the threshold of 100–200 nM (Fig. 3C, D). We categorized adrenergic MSCs into two groups based on their dose–response curves. One included possibly most robust cells (n = 21), which responded to noradrenaline with similar Ca^{2+} transients irrespective of agonist concentration (Fig. 3B, C). Another group (n = 8) united cells with somewhat irregular dose dependencies (Fig. 3D). Among them, 5 cells exhibited large (65–75%) but not maximal responses at the threshold stimulation and generated increasing Ca^{2+} transients on rising noradrenaline (Fig. 3D). Three cells generated the maximal responses at the threshold but showed irregularly varied lower responses as agonist concentration increased.

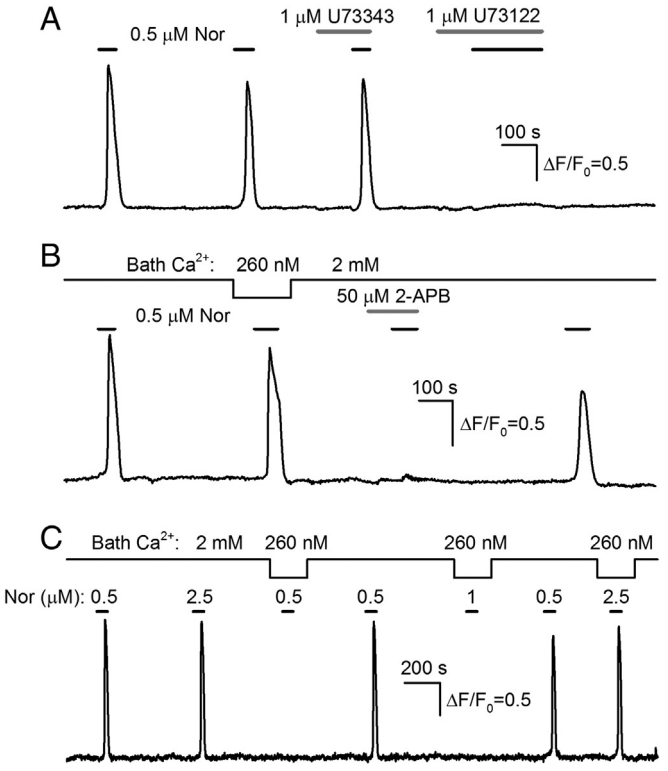

Fig. 2. Evidence for a role of the phosphoinositide cascade in noradrenaline transduction. (A) Representative effects of the PLC inhibitor U73122 (1 μM) and its much less effective analog U73343 (1 μM) on MSC responsivity to 0.5 μM noradrenaline. (B) 2-ABP (50 μM) reversibly suppressed noradrenaline responses. Notably, a given cell similarly responded to 0.5 μM noradrenaline with normal (2 mM) and reduced (260 nM) Ca^{2+} in the bath. This data and the recording presented in (C) indicate conclusively that 2-APB ruined noradrenaline transduction largely due to the inhibition of IP3-receptors rather than Ca^{2+} entry. (C) Representative recording from a cell that lost sensitivity to 0.5 μM noradrenaline at low external Ca^{2+}. With 260 nM Ca^{2+} in the bath, this cell did not respond to the agonist at 0.5 μM and 1 μM but was still responsive to 2.5 μM noradrenaline. Although the reduction of bath Ca^{2+} from 2 mM to 260 nM reversibly decreased the sensitivity of MSCs, the magnitude of noradrenaline responses was virtually independent of bath Ca^{2+}. In (A–C), 3 different cells were assayed. Extracellular Ca^{2+} was not completely removed as prolonged exposure of assayed cells to a Ca^{2+}-free solution might shorten their lifespan and inactivate them. Here and in the below figures, short lines above fluorescence traces show transient applications of indicated compounds; the time course of bath Ca^{2+} is marked by the continuous lines.

Whatever the case, characteristic of all adrenergic MSCs was that none of them exhibited small Ca^{2+} responses to noradrenaline at the threshold concentrations (Fig. 3).

One more notable feature of noradrenaline responses was that they were markedly postponed relative to a moment of agonist application. The characteristic time of response delay (τ_d, Fig. 3E) gradually decreased with noradrenaline concentration (Fig. 3F). Particularly, Ca^{2+} transients were retarded by 38–55 s at the threshold stimulation (Fig. 3E, left response), whereas the delay was reduced to 17–26 s at the concentration of 1 μM and higher (Fig. 3E, right response), albeit response magnitude was not so variable (Fig. 3E). As discussed later, two primary mechanisms may be responsible for specific dependencies of the magnitude and delay of cellular responses on agonist concentration.

3.2. Ca^{2+}-induced Ca^{2+} release as a likely contributor

A variety of diverse cells exemplify a monotonic and gradual dependence of cellular responses on agonist concentration, including those that employ the phosphoinositide cascade for coupling GPCRs to Ca^{2+} mobilization [26–28]. All-or-nothing responses of MSCs to noradrenaline (Fig. 3) could hardly be accounted for by a transduction process that involves solely PLC stimulation and IP_3 production followed by Ca^{2+} release via IP_3 receptors (Fig. 2). We therefore assumed that MSCs generated responses to noradrenaline in two consecutive steps. Initially, the agonist triggered small Ca^{2+} signal presumably gradually dependent on stimulus intensity. When exceeded the threshold, this signal was then amplified to the saturated level by a Ca^{2+}-dependent trigger. Well-documented among numerous cell types, Ca^{2+}-induced Ca^{2+} release (CICR) might serve such a role [29–31].

If this idea is correct, every noradrenaline-independent Ca^{2+} signal in the MSC cytoplasm, should it be speedy and high enough, would be converted by CICR into a noradrenaline-like Ca^{2+} response. We particularly wondered how adrenergic cells would react to a jump in cytosolic Ca^{2+} produced by photolysis of NP-EGTA. The last is a photosensitive Ca^{2+} chelator with high affinity to Ca^{2+} (Kd ~ 10^{-7} M), so that in a rising cell (~100 nm free Ca^{2+}), nearly half NP-EGTA molecules are bound to Ca^{2+} ions. The absorption of ultraviolet (UV) light by NP-EGTA disrupts the coordination sphere responsible for Ca^{2+} binding, thus liberating Ca^{2+} ions and producing a step-like increase in cytosolic Ca^{2+} [32]. In appropriate experiments, cells were loaded with both Fluo-4 and NP-EGTA, and their responses to noradrenaline and UV pulses were studied. Note that a UV laser used by us was in fact a biharmonic light source emitting at 355 nm and 532 nm. Since powerful green emission could not be completely eliminated with excitation filters, a light stimulus produced an optical artifact that was seen as a marked overshoot in an experimental recording of cell fluorescence acquired at 535 ± 20 nm.

The representative trace plotted in Fig. 4A illustrates typical Ca^{2+} signals elicited by UV flashes, durations of which were varied to produce different Ca^{2+} bursts in the MSC cytoplasm. Here and in other cases ($n = 33$), light stimuli triggered two fundamentally different types of Ca^{2+} responses. The relatively short, 2-s in the given case, UV pulse produced an optical artifact that was followed by a small Ca^{2+} jump without evident delay (Fig. 4A, response 1 and Fig. 4B, thick line). This Ca^{2+} signal exhibited exponential relaxation presumably mediated by Ca^{2+} pumps. The sequential 4-s and 6-s UV flashes elicited biphasic Ca^{2+} transients of non-proportional magnitudes (Fig. 4A). Indeed, compared to a 2-s UV pulse, one could expect 4-s and 6-s light stimuli to liberate nearly twice and three times more Ca^{2+} ions, respectively. Meanwhile, 4-s, 6-s, and 8-s flashes usually triggered the similar Ca^{2+} transients that exceeded a response to a 2-s pulse by an order of magnitude (Fig. 4A). With the exception of CICR, none of the known Ca^{2+}-dependent mechanisms could amplify and shape an initial Ca^{2+} signal produced by the NP-EGTA photolysis in such a way (Fig. 4A, response 1 vs. response 2). In addition, the representative cell (Fig. 4A) was insensitive to 50 nM noradrenaline but similarly responded to the agonist at the 0.5 μM and 1 μM concentrations. Notably, the noradrenaline responses and light responses were quite similar in their shape and magnitude (Fig. 4B, thin line and circles). Similar results were obtained with other 8 MSCs that tolerated prolonged serial stimulation with both UV and noradrenaline. The overall data are partly summarized in Fig. 4C. Here each symbol represents agonist response versus light response, both being recorded from the same cell sequentially stimulated by a 6-s UV pulse and 0.5 μM noradrenaline (Fig. 4A). The linear regression with the slope of 0.96 (solid line) satisfactorily fits the depicted data. Thus, the marked feature of adrenergic MSCs was all-or-nothing responsivity to both noradrenaline and Ca^{2+} uncaging. Besides, Ca^{2+} transients elicited by the agonist and light were very close kinetically and by magnitude.

Theoretically, Ca^{2+} uncaging could stimulate Ca^{2+}-dependent PLC [33,34]. This would result in IP_3 production and Ca^{2+} release, thereby simulating noradrenaline responses. To check such a possibility, several adrenergic MSCs ($n = 7$) loaded with NP-EGTA were subjected to Ca^{2+} uncaging in the presence of U73122. Although this PLC inhibitor expectedly rendered cells irresponsive to noradrenaline, they normally responded to UV flashes (Fig. 4D). These findings left little doubt that Ca^{2+} uncaging elicited noradrenaline-like responses exclusively by triggering CICR in the MSC cytoplasm. This inference was completely

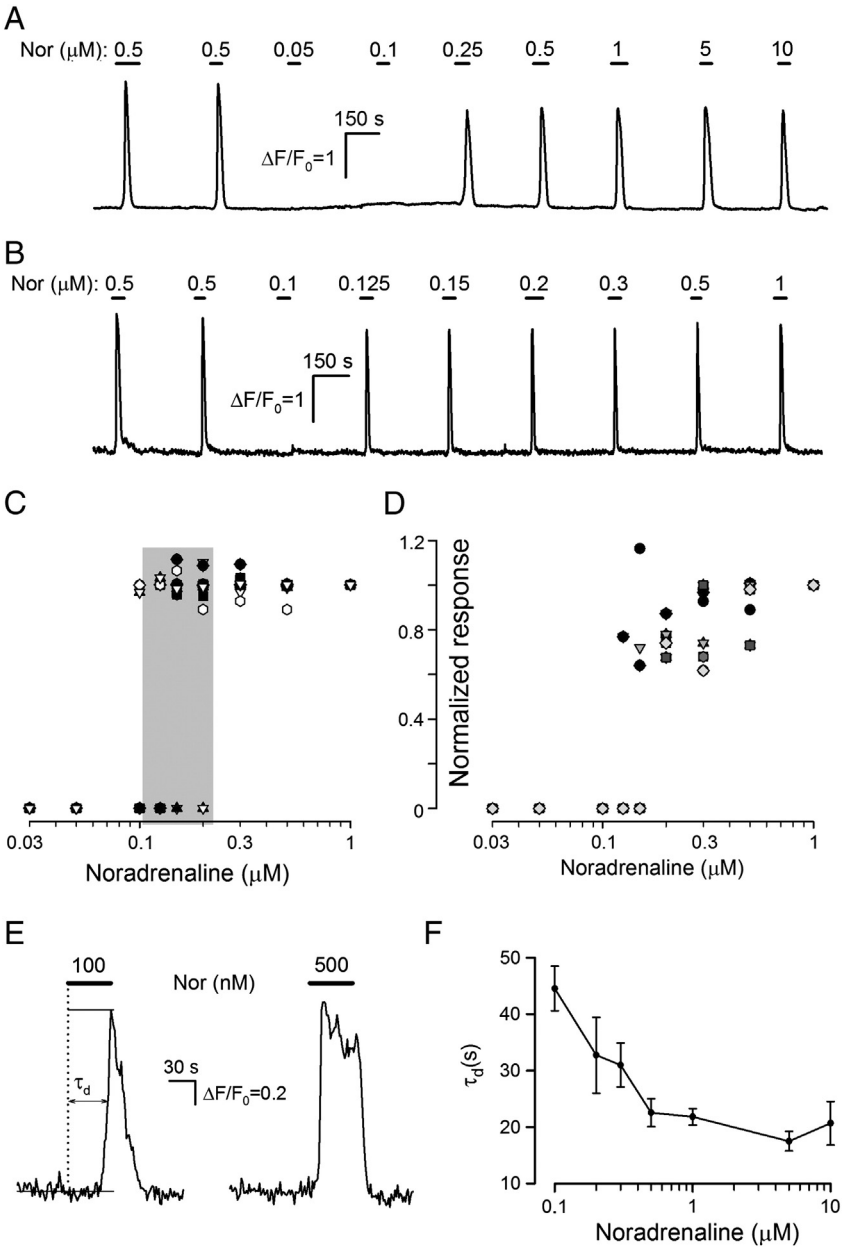

Fig. 3. Dose dependence of noradrenaline responses. (A, B) Representative recordings of intracellular Ca^{2+} in two MSCs stimulated by noradrenaline in series. Each cell was irresponsive to noradrenaline at 100 nM and lower doses but generated Ca^{2+} responses that subtly varied with agonist concentration within the 100 nM–10 μM range. (C) Superimposed dose dependences of noradrenaline responses recorded from 21 cells that exhibited small or negligible dependence of Ca^{2+} transients on noradrenaline concentration above the threshold. The last varied from cell to cell between 100 and 200 nM (gray bar). (D). Summary of recordings obtained from 8 cells showed divers and irregular dose–response dependencies. In (C, D), responses of a given cell were normalized to a response produced by 1 μM noradrenaline. Each symbol corresponds to an individual cell. (E) Representative recording of Ca^{2+} transients elicited by noradrenaline at 100 nM (threshold concentration) and 500 nM. These responses were delayed relative to the moment of agonist application by 55 s and 16 s, respectively. The characteristic time of the response delay (τ_d) was calculated as a time interval necessary for a Ca^{2+} transient to reach the half-magnitude value (left panel). (F) Dependence of response delay on noradrenaline concentration. The data are obtained from 8 different cells and presented as a mean ± S.D. (n = 5–8).

supported by independent evidence coming from the analysis of Ca^{2+} waves in MSCs (Supplementary Fig. 2S).

At the moment solely ryanodine and inositol 1,4,5-trisphosphate (IP_3) receptors, both being Ca^{2+}-gated Ca^{2+}-release channels operating in the endo/sarcoplasmic reticulum are known to mediate CICR in a variety of different cells [31,33,35]. A number of noradrenaline responsive MSCs (n = 17) were pre-incubated with 50 μM ryanodine for about 200 s. Although ryanodine receptors should have been inhibited completely under these conditions, sensitivity of such cells to noradrenaline altered insignificantly (Fig. 5A). In contrast, MSCs were rendered irresponsive by 2-APB (50 μM), an IP_3 receptor antagonist (Fig. 5A) (n = 15). Moreover, in experiments, wherein cells loaded with NP-EGTA were stimulated by both noradrenaline and UV pulses, ryanodine did not suppress responses to either of the stimuli, whereas 2-APB reversibly inhibited CICR initiated by Ca^{2+} uncaging (n = 7) (Fig. 5B). It thus appears that just IP_3 receptors are mainly responsible for CICR in adrenergic MSCs. This inference is consistent with the work by Kawano et al. [36], which found no evidence for the expression of ryanodine receptors but detected transcripts for all three IP_3 receptor isoforms in MSCs derived from the human bone marrow.

3.3. Adrenoreceptor subtypes

In light of the abovementioned functional tests, we were interested in the molecular identity of adrenoreceptors operative in MSCs. The RT-PCR analysis was performed using RNA isolated from multiple MSC

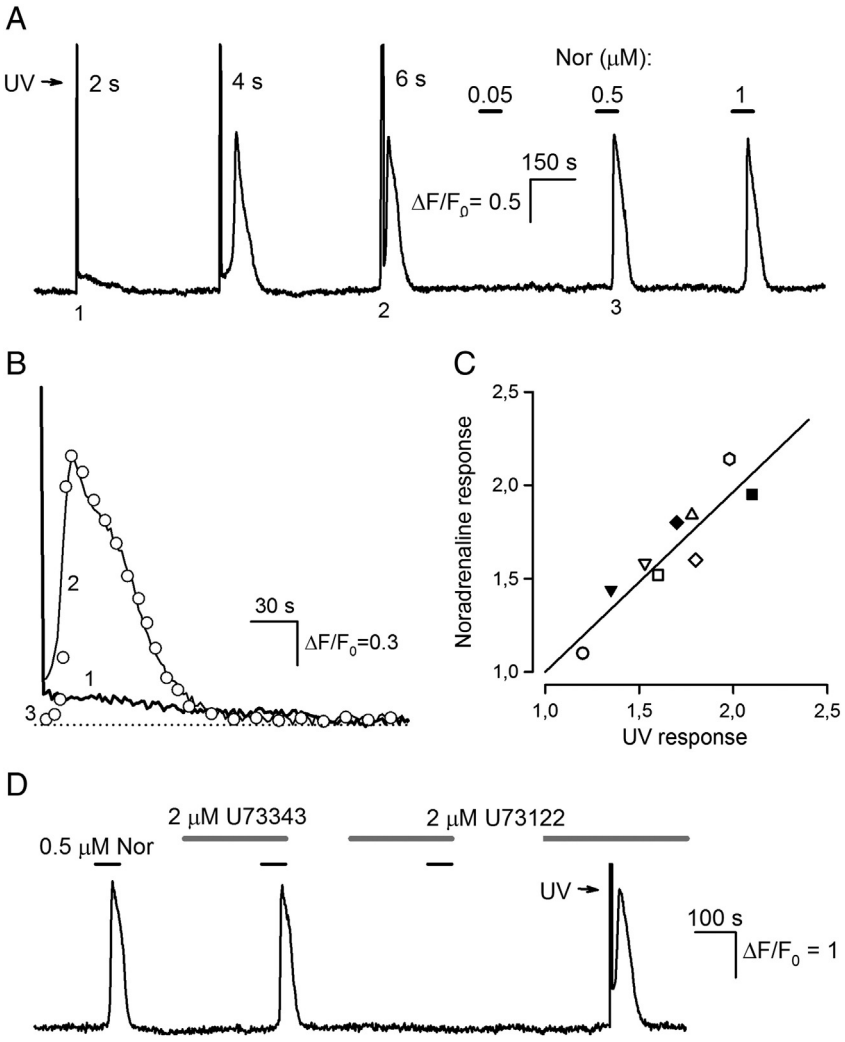

Fig. 4. Evidence for Ca^{2+}-induced Ca^{2+} release in adrenergic MSCs. (A) Responses of a NP-EGTA loaded cell to UV flashes of varied durations and to noradrenaline at the indicated concentrations. (B) Superimposition of the responses numbered as 1, 2, and 3 in (A). (C) Noradrenaline response versus light response, both being expressed as $\Delta F/F_0$. The straight line with the slope of 0.96 represents linear regression. The analyzed responses were sequentially elicited by light and 0.5 μM noradrenaline. Each symbol corresponds to the particular cell (D) PLC inhibitor U73122 dumped MSC responsiveness to noradrenaline but did not prevent noradrenaline response-like Ca^{2+} transients produced by Ca^{2+} uncaging.

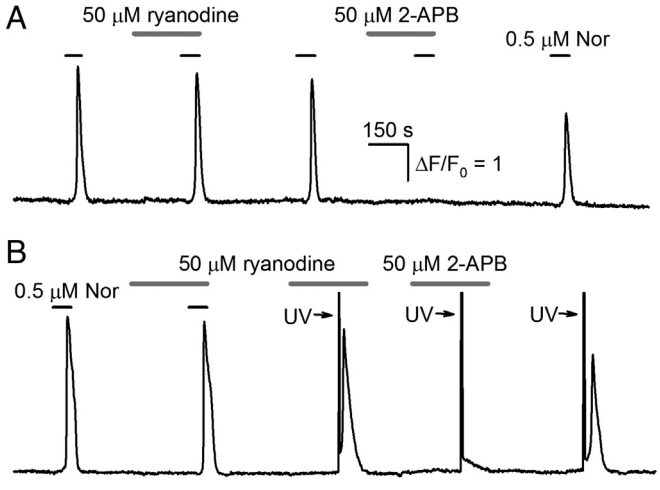

Fig. 5. Noradrenaline transduction and CICR in MSCs rely largely on IP_3 receptors. (A, B) Ryanodine receptor blockage with 50 μM ryanodine entailed an insignificant change in cell responsivity to noradrenaline and UV light. In contrast, responses to both the agonist and Ca^{2+} uncaging were completely abolished by the IP_3 receptor inhibitor 2-APB (50 μM). The traces in (A) and (B) were scaled identically.

samples that were derived from the adipose tissue of 12 different donors. Specific primers were designed based on available sequences of all 9 genes encoding human adrenoreceptors [37] (Supplementary Table 1S). It is noteworthy that all RNA samples contained transcripts for α1B-, α2A-, and β2-adrenoreceptors as well as for CD73, CD90, and CD105 (Fig. 6) that are conventionally considered as MSC markers [4,38]. The expression of α1- and α2-adrenoreceptors in MSCs was also confirmed at the protein level using subtype-specific antibodies for immunostaining. It turned out that each tested MSC colony ($n = 7$) contained a small (2–4%) subpopulation of cells exhibiting α1- and α2-like immunoreactivity (Fig. 6B, C). Although the α1-adrenoreceptor is ubiquitously involved in Ca^{2+} signaling [39], coupling of the α2 isoform to PLC and Ca^{2+} mobilization has also been documented [40]. Thus, the expression of α1B or α2A or both isoforms in a MSC responsive to noradrenaline (Fig. 2) would be quite relevant. In contrast, β2-adrenoreceptors are generally coupled by G-proteins to adenylate cyclase [41], and those should not necessarily be present in a MSC generating Ca^{2+} transients to noradrenaline. It was therefore unclear whether the detected adrenoreceptors (Fig. 6) were expressed in the same cell or there were separate MSC subpopulations distinguishable by specific expression profiles of these receptor proteins.

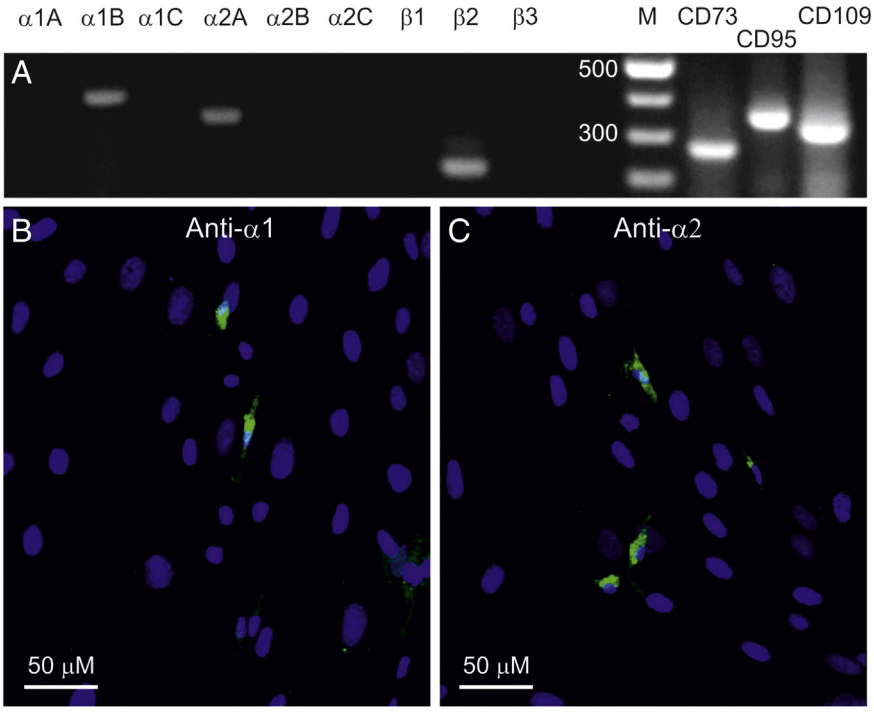

Fig. 6. Adrenoreceptors specifically expressed in MSCs. (A) Representative RT-PCR analysis of expression of human adrenoreceptors in a MSC population (10^5–10^6 cells). The detected transcripts correspond to the α1B-, α2A-, and β2-isoforms and are seen as amplicons of the expected sizes of 379, 347, and 218 bp, respectively. Apart from these adrenoreceptor transcripts, each mRNA preparation also contained transcripts for CD73 (266 bp), CD90 (344 bp), and CD105 (300 bp) conventionally considered as MSC markers. The molecular weight markers (M) were from GeneRuler 100 bp DNA Ladder (Fermentas). Their sizes (bp) are indicated by the digits at the left of the corresponding lane (M) in the presented 1.2% agarose gel stained with ethidium bromide. (B) Fluorescent imaging of a MCS colony treated with primary mouse antibody against the human α1 adrenoreceptor and stained with secondary antibody Alexa goat anti-mouse 488. (C) Fluorescent imaging of a MCS colony treated with primary rabbit antibody against the human α2-adrenoreceptor and stained with secondary antibody Alexa goat anti-rabbit 488. In (B) an (C), cells were counterstained with nuclear 4,6-diamidino-2-phenylindole. The adrenoreceptor-positive cells are greenish.

To address this issue, we performed recordings using agonists and antagonists specific for the α1-, α2-, and β-subtypes in the adrenoreceptor family. Overall, 35 noradrenaline-responsive cells were treated with phenylephrine and/or cirazoline and prazosin (α1-agonists and antagonist, respectively) as well as with guanobenz and/or B-HT 933 and yohimbine (α2-agonists and antagonist, respectively). Most of them (29 cells, 83%) were irresponsive to phenylephrine (1–10 μM), and their noradrenaline responses were not inhibited by 10 μM prazosin. In contrast, guanobenz (50 μM) and B-HT 933 (10 μM) were quite effective (Fig. 7A, B). Moreover, 1 μM yohimbine dumped cellular responses to noradrenaline and guanobenz (Fig. 7A, B). Six cells (17%) were sensitive to both 10 μM phenylephrine and 10 μM guanobenz (Fig. 7C). These findings indicate that the α2-subtype, evidently α2A is the dominant adrenoreceptor, although in a minor MSC subpopulation, both α1- and α2-isoforms could be involved in adrenergic transduction.

In a number of experiments, we aimed at β-adrenoreceptors by treating noradrenaline-responsive MSCs with the β-agonist isoproterenol and β-antagonist alprenolol. Isoproterenol (1–10 μM) as such negligibly affected intracellular Ca^{2+} at rest and insignificantly modulated cell responsivity to noradrenaline (n = 9) (Fig. 7D). Surprising in light of this finding was that all assayed cells became irresponsive in the presence of alprenolol (5–10 μM) that acted reversibly (n = 16) (Fig. 7D). At the moment we have no validated explanation of this phenomenon. In any event, the described effects of the subtype specific agonists and antagonists (Fig. 7) can be considered as an indication that all adrenoreceptor isoforms detected by RT-PCR are functional in MSCs. Moreover, the data provide functional evidence that α2- and β2-subtypes are co-expressed.

4. Discussion

Here we studied Ca^{2+} signaling in mesenchymal stromal cells (MSCs) derived from the human adipose tissue. As a whole, a population of cultured MSCs exhibited functional heterogeneity in terms of their responsivity to a variety of GPCR agonists, including ATP, GABA, noradrenaline and some others. Although all first messengers tested were effective, only a relatively small group of MSCs was specifically responsive to the particular agonist (Fig. 1). Consistently with previous reports (reviewed in [9]), some MSCs that were basically irresponsive to the agonists generated spontaneous Ca^{2+} oscillations under our recording conditions (Fig. 1).

The present work was specifically focused on adrenergic MSCs. The physiological analysis, RT-PCR, and immunostaining revealed the functional expression of α1B-, α2A-, and β2-adrenoreceptors (Figs. 6 and 7). The experiments with the subtype specific agonists pointed at the α2A-isoform as a key adrenoreceptor endowing MSCs with sensitivity to noradrenaline, although α1B-isoform also might be involved (Fig. 7). The β-agonist isoproterenol negligibly affected intracellular Ca^{2+} in resting MSCs and their sensitivity to noradrenaline (Fig. 7D), indicating that β2-adrenoreceptors are not directly coupled to Ca^{2+} mobilization in MSCs. In light of this finding, surprising was that cells became insensitive to noradrenaline in the presence of alprenolol (Fig. 7D) that normally antagonizes to G-protein signaling initiated by classical agonists of β-adrenoreceptors. Although underlying mechanism(s) remains to be elucidated, theoretically, the inhibitory effects of alprenolol could be rationally explained based on the concept of biased agonism [42–44]. Indeed, this compound has been documented to stimulate coupling of β1- and β2-adrenoreceptors to ERK1/2 kinase via β-arrestin [45,46]. It is therefore possible that alprenolol

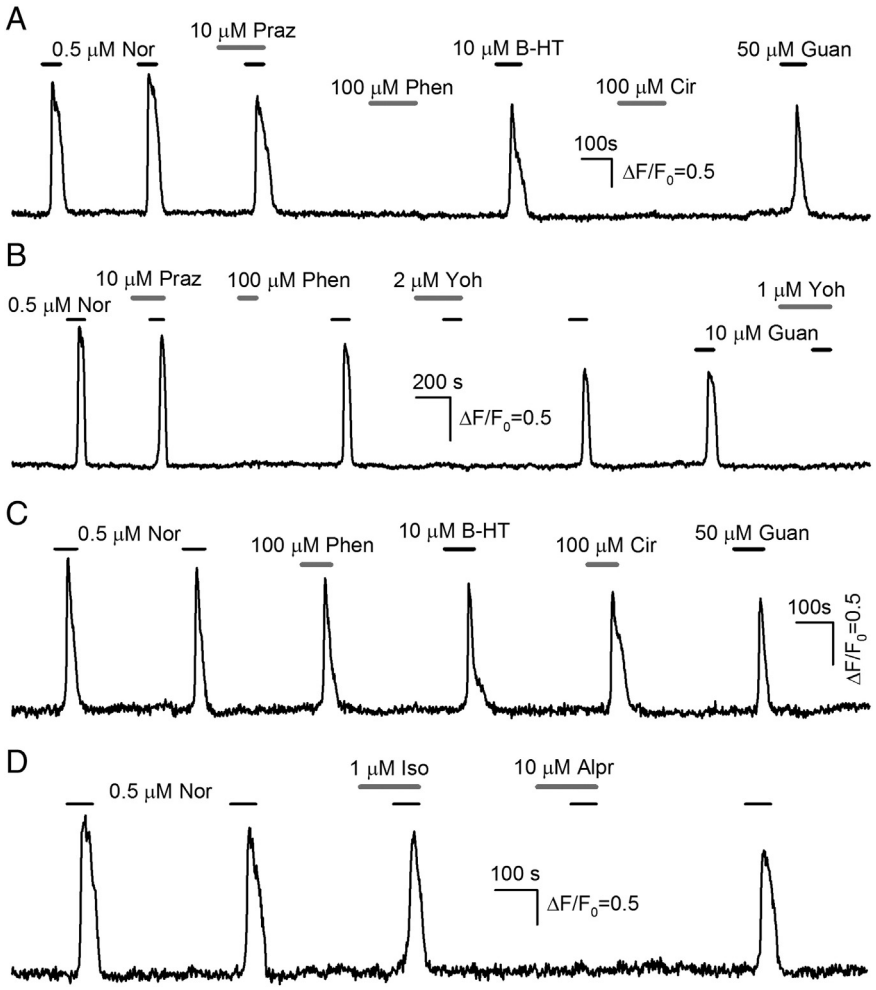

Fig. 7. Sensitivity of MSC to various adrenergic agonists and antagonists. (A, B) Most (83%) of noradrenaline-sensitive MSCs also responded to the α2-receptor agonists guanobenz and B-HT 933 but not to phenylephrine and cirazoline, α1-receptor agonists. Consistently, Ca^{2+} responses to noradrenaline and guanobenz were markedly diminished in the presence of yohimbine, an α2 antagonist, while the α1 antagonist prazosin was ineffective. (C) Small subpopulation (17%) of noradrenaline-sensitive cells responded to both α2 and α1 agonists. (D) Representative recording of intracellular Ca^{2+} in a cell stimulated by noradrenaline in control and in the presence of the β-agonist isoproterenol and β-antagonist alprenolol.

affected noradrenaline responses (Fig. 7D) by stimulating β2-adrenoreceptors as a biased agonist capable of initiating β-arrestin signaling, currently unidentified in MSCs. This arrestin-dependent pathway might interfere with the adrenergic transduction machinery, rendering MSCs irresponsive.

The body of evidence implicates the classical phosphoinositide cascade in mediating adrenergic signaling in MSCs. In particular, noradrenaline responses were specifically suppressed by the PLC inhibitor U73122 and IP_3 receptor blocker 2-APB (Fig. 2). Hence, PLC stimulation, IP_3 production, and IP_3 receptor activation appear to be obligatory events in noradrenaline transduction. Yet, the reduction of bath Ca^{2+} from 2 mM to 260 nM subtly affected the kinetics and magnitude of MSC responses to saturating noradrenaline but rendered cells less sensitive to the agonist at intermediate concentrations (Fig. 2B, C). To all appearance, Ca^{2+} entry plays a minor role in adrenergic Ca^{2+} signaling that relies largely on Ca^{2+} exchange between Ca^{2+} stores and the MSC cytoplasm. It is currently unclear what mechanism(s) could underlie the decreased MSC sensitivity to adrenergic agonists at low bath Ca^{2+}. Note however that our preliminary results point at extracellular Ca^{2+} sensing receptor (CASR) to be expressed in MSCs (data not shown). It is not unlikely that as a bath Ca^{2+} sensor, just CASR is responsible for the Ca^{2+}-dependent modulation of MSC sensitivity to noradrenaline (Fig. 2C).

The responsivity of adrenergic MSCs followed a peculiar dose dependence: noradrenaline never elicited small or intermediate responses but initiated Ca^{2+} transients basically being large and quite similar at all concentrations above the threshold. A number of MSCs exhibited robust noradrenaline responses within 30–40 min, thus allowing for the reliable assay of their responsivity over a wide range of agonist concentrations (Fig. 3A, B). These cells exhibited step-like dose dependences with the threshold noradrenalin concentration of 100–200 nM (Fig. 3C). In many cases, responses of MSCs to adrenergic agonists varied with time and/or were liable to rundown. Presumably, such cells showed somewhat irregular dose–response curves like those depicted in Fig. 3D. Even so, all obtained dose dependencies evidence for the all-or-nothing character of noradrenaline responsivity.

Amazingly, the key features of noradrenaline responses, including the all-or-nothing behavior, were correctly simulated with Ca^{2+} uncaging, provided that it produced sufficient Ca^{2+} bursts in the MSC cytoplasm (Fig. 4). In more detail, short UV pulses elicited relatively small Ca^{2+} transients that relaxed monotonically. In contrast, more prolonged light stimuli, which liberated sufficient quantity of Ca^{2+} ions, triggered biphasic Ca^{2+} signals that were rather similar to noradrenaline responses by kinetics and magnitude (Fig. 4A, B). Based on these findings, we inferred that adrenergic transduction occurs in two key steps. Initially, an adrenergic agonist produces a relatively small

Ca^{2+} signal, which is most likely to rise gradually with stimulus intensity, given that the experimentally recorded Ca^{2+} transients were delayed relative to noradrenaline application in a dose-dependent way (Fig. 3E, F). When reaching the threshold level, this initial Ca^{2+} signal triggers a regenerative process mediated by the CICR mechanism that eventually produces a global Ca^{2+} response of the maximal value (Fig. 3A, B).

Although qualitatively, the above point of view integrates well the diverse findings of the present work, two apparent inconsistencies should be noted. The first relates to the nature of all-or-nothing Ca^{2+} signals elicited by adrenergic agonists. One could expect that an initial agonist-dependent Ca^{2+} rise preceding CISR should have been present in recording traces (Fig. 3A, B), as is the case with Ca^{2+} signals initiated by Ca^{2+} uncaging (Figs. 4A, 5). It is noteworthy that even confocal microscopy did not allow us to achieve high enough spatial/temporal resolution to separate a triggering noradrenaline-dependent Ca^{2+} signal from CISR in the MSC cytoplasm (data not shown). Unlike Ca^{2+} uncaging that elicited a global and therefore resolvable Ca^{2+} rise (Fig. 4A), an initial Ca^{2+} response to noradrenaline was most likely generated in a very narrow cytosolic region near the plasma membrane. Given that Fura-4 and other Ca^{2+} dyes uniformly distributed in the cell cytoplasm do not allow for detecting such signals, genetically targetable Ca^{2+} indicators [47] may be necessary to address this problem.

Another point is that the effects of ryanodine and 2-APB on noradrenaline and UV light responses (Figs. 2, 5A) favor IP_3 receptors to be largely, if not exclusively, responsible for CICR in adrenergic MSCs. Furthermore, the negligible effects of the PLC inhibitor U73122 on UV responses (Fig. 4D) suggest that CICR in MSCs does not require IP_3 production. It thus appears that adrenergic transduction implicates IP_3 receptors in two fundamentally different signaling events, one requiring PLC stimulation and another being PLC-independent. Note however that intracellular signaling involves distinct subpopulations of IP_3 receptors that differ in their sensitivity to IP_3 and Ca^{2+} and may operate in physically separated Ca^{2+} compartments [31,48]. The necessary functional specialization of IP_3 receptors can also be achieved with the assistance of the Ca^{2+}-binding protein CIB1 that stimulates all three IP_3R isoforms in a Ca^{2+}-dependent manner even in the absence of IP_3 [49]. Thus, under certain conditions, IP_3 receptor-mediated CICR may not require IP_3 production (Fig. 4D).

5. Conclusions

Based on the main finding of the present study, we propose the following minimal model of adrenergic transduction in MSCs (Fig. 8). Adrenergic receptors are coupled via certain G-proteins, PLC, and IP_3 production to IP_3 receptors (IP_3R_{grad}) to release Ca^{2+} from designated Ca^{2+} store, resulting in an initial, presumably gradual Ca^{2+} signal. The last stimulates specialized IP_3 receptors (IP_3R_{CICR}) operative in separated Ca^{2+} store, thus triggering CICR that finalizes Ca^{2+} responses to adrenergic agonists. Finally, note that in a given MSC preparation, the number of cells responsive to Ca^{2+} uncaging with CICR (Fig. 4A) usually exceeded the number of cells responsive to adrenergic agonists. This suggests that the CICR mechanism not only mediates adrenergic transduction but may also be involved in Ca^{2+} signaling initiated in MSCs by other first messengers (Fig. 1A).

Acknowledgements

This work was supported by the Russian Academy of Sciences (Program "Mechanisms of integration of molecular systems mediating physiological functions") and the Russian Foundation for Basic Research (grants 13-04-0913-a, 13-04-40082-H, 14-04-01711-a) and the Russian Science Foundation (grants 14-14-00687, 14-15-00439).

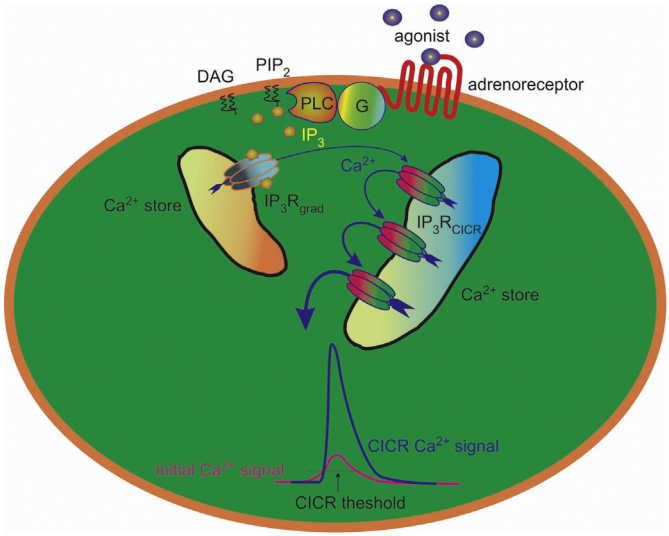

Fig. 8. Minimal model of adrenergic transduction in MSCs. The adrenoreceptor is coupled by a G-protein to PLC, so that an adrenergic agonist initiates PIP_2 hydrolysis and IP_3 production followed by stimulation of a related IP_3 receptor (IP_3R_{grad}). Next, Ca^{2+} is released from Ca^{2+} store, producing an initial Ca^{2+} signal, gradually rising with agonist concentration (red curve). As soon as this signal reaches the threshold level (dotted line), one stimulates IP_3 receptors of another type (IP_3R_{CICR}) in separated Ca^{2+} store and triggers a regenerative process via CICR. This results in a much larger Ca^{2+} transient of a shape and magnitude virtually independent of agonist concentration (blue curve).

Appendix A. Supplementary data

Supplementary data to this article can be found online at http://dx.doi.org/10.1016/j.bbamcr.2014.05.002.

References

[1] F.M. Watt, B.L. Hogan, Out of Eden: stem cells and their niches, Science 287 (2000) 1427–1430.
[2] L. da Silva Meirelles, P.C. Chagastelles, N.B. Nardi, Mesenchymal stem cells reside in virtually all post-natal organs and tissues, J. Cell Sci. 119 (2006) 2204–2213.
[3] W. Wagner, A.D. Ho, Mesenchymal stem cell preparations — comparing apples and oranges, Stem Cell Rev. 3 (2007) 239–248.
[4] N.I. Kalinina, V.Yu. Sysoeva, K.A. Rubina, Ye.V. Parfenova, V.A. Tkachuk, Mesenchymal stem cells in tissue growth and repair, Acta Nat. 3 (2011) 30–37.
[5] D.G. Phinney, Functional heterogeneity of mesenchymal stem cells: implications for cell therapy, J. Cell. Biochem. 113 (2012) 2806–2812.
[6] N. Tremain, J. Korkko, D. Ibberson, G.C. Kopen, C. DiGirolamo, D.G. Phinney, MicroSAGE analysis of 2,353 expressed genes in a single cell-derived colony of undifferentiated human mesenchymal stem cells reveals mRNAs of multiple cell lineages, Stem Cells 19 (2001) 408–418.
[7] M. Baddoo, K. Hill, R. Wilkinson, D. Gaupp, C. Hughes, G.C. Kopen, D.G. Phinney, Characterization of mesenchymal stem cells isolated from murine bone marrow by negative selection, J. Cell. Biochem. 89 (2003) 1235–1249.
[8] S.V. Boregowda, D.G. Phinney, MSCs: paracrine effects, in: P. Hematti, A. Keating (Eds.), Mesenchymal Stromal Cells: Biology and Clinical Applications, Springer, New York, 2013, pp. 145–167.
[9] B. Ye, Ca^{2+} oscillations and its transporters in mesenchymal stem cells, Physiol. Res. 59 (2010) 323–329.
[10] S. Pillozzi, A. Becchetti, Ion channels in hematopoietic and mesenchymal stem cells, Stem Cells Int. (2012) 217910.
[11] C. Leclerc, I. Néant, M. Moreau, The calcium: an early signal that initiates the formation of the nervous system during embryogenesis, Front. Mol. Neurosci. 5 (2012) 3.
[12] R.R. Resende, L.M. Andrade, A.G. Oliveira, E.S. Guimarães, S. Guatimosim, M.F. Leite, Nucleoplasmic calcium signaling and cell proliferation: calcium signaling in the nucleus, Cell Commun. Signal. 11 (2013) 14.
[13] S.S. Rosenberg, N.C. Spitzer, Calcium signaling in neuronal development, Cold Spring Harb. Perspect. Biol. 3 (2011) a004259.
[14] D.J. Blackiston, K.A. McLaughlin, M. Levin, Bioelectric controls of cell proliferation ion channels, membrane voltage and the cell cycle, Cell Cycle 8 (2009) 3527–3536.
[15] S. Sundelacruz, M. Levin, D.L. Kaplan, Role of membrane potential in the regulation of cell proliferation and differentiation, Stem Cell Rev. Rep. 5 (2009) 231–246.
[16] A. Becchetti, Ion channels and transporters in cancer. 1. Ion channels and cell proliferation in cancer, Am. J. Physiol. Cell Physiol. 301 (2011) 255–265.
[17] E.K. Hoffmann, I.H. Lambert, S.F. Pedersen, Physiology of cell volume regulation in vertebrates, Physiol. Rev. 89 (2009) 193–277.
[18] V.A. Cuddapah, H. Sontheimer, Ion channels and transporters in cancer. 2. Ion channels and the control of cancer cell migration, Am. J. Physiol. 301 (2011) 541–549.

[19] M. Levite, L. Cahalon, A. Peretz, R. Hershkoviz, A. Sobko, A. Ariel, R. Desai, B. Attali, O. Lider, Extracellular K^+ and opening of voltage-gated potassium channels activate T cell integrin function: physical and functional association between Kv1.3 channels and β1 integrins, J. Exp. Med. 191 (2000) 1167–1176.
[20] J.-F. Wei, L. Wei, X. Zhou, Z.Y. Lu, K. Francis, X.Y. Hu, Y. Liu, W.C. Xiong, X. Zhang, N.L. Banik, S.S. Zheng, S.P. Yu, Formation of Kv2.1-FAK complex as a mechanism of FAK activation, cell polarization and enhanced motility, J. Cell. Physiol. 217 (2008) 544–557.
[21] S. Pillozzi, M.F. Brizzi, P.A. Bernabei, B. Bartolozzi, L. Caporale, V. Basile, V. Boddi, L. Pegoraro, A. Becchetti, A. Arcangeli, VEGFR-1 (FLT-1), β1 integrin, and hERG K^+ channel for a macromolecular signaling complex in acute myeloid leukemia: role in cell migration and clinical outcome, Blood 110 (2007) 1238–1250.
[22] P. Cidad, L. Jimenez-Perez, D. Garcia-Arribas, E. Miguel-Velado, S. Tajada, C. Ruiz-McDavitt, J.R. Lopez-Lopez, M.T. Perez-Garcia, Kv1.3 channels can modulate cell proliferation during phenotypic switch by an ion-flux independent mechanism, Arterioscler. Thromb. Vasc. Biol. 32 (2012) 1299–1307.
[23] S.-Z. Xu, F. Zeng, G. Boulay, C. Grimm, C. Harteneck, D.J. Beech, Block of TRPC5 channels by 2-aminoethoxydiphenyl borate: a differential, extracellular and voltage-dependent effect, Br. J. Pharmacol. 145 (2005) 405–414.
[24] T. Mustafa, J. Walsh, M. Grimaldi, L.E. Eiden, PAC1hop receptor activation facilitates catecholamine secretion selectively through 2-APB-sensitive Ca^{2+} channels in PC12 cells, Cell. Signal. 22 (2010) 1420–1426.
[25] C. Harteneck, M. Gollasch, Pharmacological modulation of diacylglycerol-sensitive TRPC3/6/7 channels, Curr. Pharm. Biotechnol. 12 (2011) 35–41.
[26] K.A. Berg, W.P. Clarke, C. Sailstad, A. Saltzman, S. Maayani, Signal transduction differences between 5-hydroxytryptamine type 2A and type 2C receptor systems, Mol. Pharmacol. 46 (1994) 477–484.
[27] C. Petrel, A. Kessler, P. Dauban, R.H. Dodd, D. Rognan, M. Ruat, Positive and negative allosteric modulators of the Ca^{2+}-sensing receptor interact within overlapping but not identical binding sites in the transmembrane domain, J. Biol. Chem. 279 (2004) 18990–18997.
[28] S.G. Baryshnikov, O.A. Rogachevskaja, S.S. Kolesnikov, Calcium signaling mediated by P2Y receptors in mouse taste cells, J. Neurophysiol. 90 (2003) 3283–3294.
[29] M.J. Berridge, M.D. Bootman, H.L. Roderick, Calcium signaling: dynamics, homeostasis and remodeling, Nat. Rev. Mol. Cell Biol. 4 (2003) 517–529.
[30] D.E. Clapham, Calcium signaling, Cell 131 (2007) 1047–1058.
[31] M. Iino, Spatiotemporal dynamics of Ca^{2+} signaling and its physiological roles, Proc. Jpn. Acad. Ser. B. Phys. Biol. Sci. 86 (2010) 244–256.
[32] G.C. Ellis-Davies, Caged compounds: photorelease technology for control of cellular chemistry and physiology, Nat. Methods 4 (2007) 619–628.
[33] G. Dupont, L. Combettes, L. Leybaert, Calcium dynamics: spatio-temporal organization from the subcellular to the organ level, Int. Rev. Cytol. 261 (2007) 193–245.
[34] J.B. Park, C.S. Lee, J.H. Jang, J. Ghim, Y.J. Kim, S. You, D. Hwang, P.-G. Suh, S.H. Ryu, Phospholipase signalling networks in cancer, Nat. Rev. Cancer 12 (2012) 782–792.
[35] E.M. Kawamoto, C. Vivar, S. Camandola, Physiology and pathology of calcium signaling in the brain, Front. Pharmacol. 3 (2012) 61.
[36] S. Kawano, S. Shoji, S. Ichiose, K. Yamagata, M. Tagami, M. Hiraoka, Characterization of Ca^{2+} signaling pathways in human mesenchymal stem cells, Cell Calcium 32 (2002) 165–174.
[37] S. Guimaraes, D. Moura, Vascular adrenoceptors: an update, Pharmacol. Rev. 2 (2001) 319–356.
[38] H.K. Salem, C. Thiemermann, Mesenchymal stromal cells: current understanding and clinical status, Stem Cells 28 (2010) 585–596.
[39] S. Cotecchia, The α_1-adrenergic receptors: diversity of signaling networks and regulation, J. Recept. Signal Transduct. Res. 30 (2010) 410–419.
[40] C. Cottingham, H. Chen, Y. Chen, Y. Peng, Q. Wang, Genetic variations of a2-adrenergic receptors illuminate the diversity of receptor functions, in: Q. Wang (Ed.), Advances in Adrenergic Receptor Biology, Academic Press, San Diego, 2011, pp. 162–190.
[41] G.S. Lynch, J.G. Ryall, Role of β-adrenoceptor signaling in skeletal muscle: implications for muscle wasting and disease, Physiol. Rev. 88 (2008) 729–767.
[42] S.K. Shenoy, M.T. Drake, C.D. Nelson, D.A. Houtz, K. Xiao, S. Madabushi, E. Reiter, R.T. Premont, O. Lichtarge, R.J. Lefkowitz, β-Arrestin-dependent, G protein-independent ERK1/2 activation by the β2 adrenergic receptor, J. Biol. Chem. 281 (2006) 1261–1273.
[43] C.B. Patel, N. Noor, H.A. Rockman, Functional selectivity in adrenergic and angiotensin signaling systems, Mol. Pharmacol. 78 (2010) 983–992.
[44] S. Rajagopal, K. Rajagopal, R.J. Lefkowitz, Teaching old receptors new tricks: biasing seven-transmembrane receptors, Nat. Rev. Drug Discov. 9 (2010) 373–386.
[45] I.-M. Kim, D.G. Tilley, J. Chen, N.C. Salazar, E.J. Whalen, J.D. Violin, H.A. Rockman, β-Blockers alprenolol and carvedilol stimulate β-arrestin-mediated EGFR transactivation, Proc. Natl. Acad. Sci. U. S. A. 105 (2008) 14555–14560.
[46] S. Coffa, M. Breitman, S.M. Hanson, K. Callaway, S. Kook, K.N. Dalby, V.V. Gurevich, The effect of arrestin conformation on the recruitment of c-Raf1, MEK1, and ERK1/2 activation, PLoS One 6 (2011) e28723.
[47] A.E. Palmer, R.Y. Tsien, Measuring calcium signaling using genetically targetable fluorescent indicators, Nat. Protoc. (2006) 1057–1065.
[48] K. Kiselyov, D.M. Shin, S. Muallem, Signalling specificity in GPCR-dependent Ca^{2+} signaling, Cell. Signal. 15 (2003) 243–253.
[49] C. White, J. Yang, M.J. Monteiro, J.K. Foskett, CIB1, a ubiquitously expressed Ca^{2+}-binding protein ligand of the InsP3 receptor Ca^{2+} release channel, J. Biol. Chem. 281 (2006) 20825–20833.